

Are your MRI contrast agents cost-effective?

Learn more about generic Gadolinium-Based Contrast Agents.



**FRESENIUS
KABI**

caring for life

AJNR















This information is current as
of April 18, 2024.

**Diffusion Characteristics of Pediatric Diffuse
Midline Gliomas with Histone H3-K27M
Mutation Using Apparent Diffusion
Coefficient Histogram Analysis**

M.S. Aboian, E. Tong, D.A. Solomon, C. Kline, A. Gautam,
A. Vardapetyan, B. Tamrazi, Y. Li, C.D. Jordan, E. Felton,
B. Weinberg, S. Braunstein, S. Mueller and S. Cha

AJNR Am J Neuroradiol published online 6 November 2019
<http://www.ajnr.org/content/early/2019/11/06/ajnr.A6302>

Diffusion Characteristics of Pediatric Diffuse Midline Gliomas with Histone H3-K27M Mutation Using Apparent Diffusion Coefficient Histogram Analysis

 M.S. Aboian,  E. Tong,  D.A. Solomon,  C. Kline,  A. Gautam,  A. Vardapetyan,  B. Tamrazi,  Y. Li,  C.D. Jordan,  E. Felton,  B. Weinberg,  S. Braunstein,  S. Mueller, and  S. Cha



ABSTRACT

BACKGROUND AND PURPOSE: Diffuse midline gliomas with histone H3 K27M mutation are biologically aggressive tumors with poor prognosis defined as a new diagnostic entity in the 2016 World Health Organization Classification of Tumors of the Central Nervous System. There are no qualitative imaging differences (enhancement, border, or central necrosis) between histone H3 wild-type and H3 K27M-mutant diffuse midline gliomas. Herein, we evaluated the utility of diffusion-weighted imaging to distinguish H3 K27M-mutant from histone H3 wildtype diffuse midline gliomas.

MATERIALS AND METHODS: We identified 31 pediatric patients (younger than 21 years of age) with diffuse gliomas centered in midline structures that had undergone assessment for histone H3 K27M mutation. We measured ADC within these tumors using a voxel-based 3D whole-tumor measurement method.

RESULTS: Our cohort included 18 infratentorial and 13 supratentorial diffuse gliomas centered in midline structures. Twenty-three (74%) tumors carried H3-K27M mutations. There was no difference in ADC histogram parameters (mean, median, minimum, maximum, percentiles) between mutant and wild-type tumors. Subgroup analysis based on tumor location also did not identify a difference in histogram descriptive statistics. Patients who survived <1 year after diagnosis had lower median ADC ($1.10 \times 10^{-3} \text{ mm}^2/\text{s}$; 95% CI, 0.90–1.30) compared with patients who survived >1 year ($1.46 \times 10^{-3} \text{ mm}^2/\text{s}$; 95% CI, 1.19–1.67; $P < .06$). Average ADC values for diffuse midline gliomas were $1.28 \times 10^{-3} \text{ mm}^2/\text{s}$ (95% CI, 1.21–1.34) and $0.86 \times 10^{-3} \text{ mm}^2/\text{s}$ (95% CI, 0.69–1.01) for hemispheric glioblastomas with $P < .05$.

CONCLUSIONS: Although no statistically significant difference in diffusion characteristics was found between H3-K27M mutant and H3 wildtype diffuse midline gliomas, lower diffusivity corresponds to a lower survival rate at 1 year after diagnosis. These findings can have an impact on the anticipated clinical course for this patient population and offer providers and families guidance on clinical outcomes.

Diffuse midline glioma with histone H3-K27M mutation is a new class of gliomas that was defined by the 2016 World Health Organization Classification.^{1,2} These tumors arise within

the midline of the CNS, most commonly within the pons, thalamus, or spinal cord. Patients with histone H3-K27M mutant gliomas have worse survival compared with those with wild-type tumors,^{3,4} but there are no currently known imaging markers that can distinguish tumors with histone H3-K27M mutations from wild-type tumors.⁵ Tumor size, infiltrative appearance on


Received August 11, 2017; accepted after revision August 31, 2019.


From the Department of Radiology and Biomedical Imaging (M.S.A.), Yale School of Medicine, New Haven, Connecticut; Department of Radiology (E.T.), Stanford University, Stanford, California; Division of Neuropathology (D.A.S.), Department of Pathology, Departments of Radiology (Y.L., C.D.J., S.C.), Radiation Oncology (S.B.), Neurological Surgery (S.M.), and Neurology (S.M.), and Division of Pediatric Hematology/Oncology (C.K., E.F., S.M.), Department of Pediatrics, University of California, San Francisco, California; Johns Hopkins University (A.G.), Baltimore, Maryland; University of California Berkeley (A.V.), Berkeley, California; Department of Radiology (B.T.), Children's Hospital Los Angeles, Los Angeles, California; and Department of Neuroradiology (B.W.), Emory University, Atlanta, Georgia.

Mariam Aboian was funded by American Society of Neuroradiology Fellow Award 2018 and the National Institutes of Health T32 Grant 5T32EB001631-12. Elizabeth Tong was funded by National Institutes of Health T32 Grant 5T32EB001631-12. David A. Solomon is funded by the NIH Director's Early Independence Award from the National Institutes of Health, Office of the Director (DP5 OD021403). Cassie Kline was funded by National Institutes of Health National Center for Advancing Translational Sciences University of California, San Francisco—Clinical and Translational Science Grant KL2TR000143.

Paper previously presented as a podium presentation at: Annual Meeting of the American Society of Neuroradiology, April 22–27, 2017; Long Beach, California. We also presented it in abstract format at: Annual Meeting of the Society of Neuro-Oncology, November 16–19, 2017; San Francisco, California. American College of Radiology/Association of University Radiologists, Research Scholar Award, May 8–11, 2017; Hollywood, Florida.

Please address correspondence to Mariam Aboian, MD, PhD, Department of Radiology and Biomedical Imaging, Yale University School of Medicine, 789 Howard Avenue (CB30), PO Box 208042, New Haven, CT 06520; e-mail: mariam.aboian@yale.edu

 Indicates open access to non-subscribers at www.ajnr.org

 Indicates article with supplemental on-line tables.

<http://dx.doi.org/10.3174/ajnr.A6302>

FLAIR imaging, mass effect, enhancement characteristics, presence of necrosis, and pattern of disease recurrence have previously been shown to be no different between wild-type and histone H3-K27M mutant tumors.⁵

ADC histogram analysis is a technique that has been used to distinguish different pediatric tumor types, including histologically distinct posterior fossa tumors.^{6,7} In pediatric diffuse intrinsic pontine gliomas, ADC histogram analysis identified lower ADC values correlated with worse patient outcomes.^{6,7} In adult patients, ADC histogram analysis has been used to predict tumor response to antiangiogenic therapy.⁸⁻¹⁰

In the current study, we completed ADC histogram analysis using a cohort of patients with diffuse midline gliomas located within the pons, cerebellopontine angle/fourth ventricle, and thalamus who have been tested for the histone H3-K27M mutation via immunohistochemistry. We aimed to identify differences in imaging diffusion characteristics that can discriminate between wild-type diffuse midline gliomas and those carrying histone H3-K27M mutations.

MATERIALS AND METHODS

We completed retrospective chart review to identify a cohort of pediatric patients (younger than 21 years of age) with diffuse midline gliomas who were tested for histone H3-K27M mutation based on University of California San Francisco institutional tumor board review. This study was reviewed and approved by University of California San Francisco Institutional Review Board. Inclusion criteria required for consideration of statistical analysis were the following: 1) the presence of a diffuse midline glioma, 2) available pathologic testing for the presence of histone H3-K27M mutation, and 3) completion of prebiopsy MR imaging with DWI sequences of sufficient quality to perform independent ADC map calculation.

Independent ADC maps were generated for all patients with DWI sequences using Osirix/Horos software (<https://horosproject.org>) and an ADC plugin (<http://web.stanford.edu/~bah/software/ADCmap/versions.html>).

Histologic Review

Tumor tissue was fixed in formalin and embedded in paraffin for analysis by our institution's neuropathologists. The University of California, San Francisco Neuropathology BTRC Biomarkers Laboratory performed immunohistochemistry for the presence of histone H3-K27M mutant tails with the ABE419 antibody (EMB Milipore, Billerica, Massachusetts), as previously described.²

Imaging Protocol

MR imaging of the brain was performed on either 1.5T or 3T clinical scanners. Axial DWI sequences were generated at b-values of 0 and 1000 s/mm² at TR/TE = 7000/60 ms, 5-mm, gap = zero, 3–6 orthogonal diffusion gradient directions. ADC maps were generated independently using the Osirix/Horos ADC plugin. Tumor segmentation was performed manually by a neuroradiology fellow (M.S.A.) and generated 3D ROIs using FLAIR images. The ROI was coregistered with ADC maps, and borders were checked side by side with FLAIR images to ensure correct

Patient demographics

	All Patients (n = 31)	Histone H3-K27M (n = 23)	Histone H3 Wild-Type (n = 8)
Male	22	14	8
Age (mean) (range) (yr)	9.8 (0.45–21.7)	8.9 (0.45–19.3)	12.5 (0.68–21.7)
Tumor location			
Pons/vermis/ 4th ventricle	21	17	4
Thalamus	7	5	2
Tectum	2	0	2
Subcallosal	1	1	0

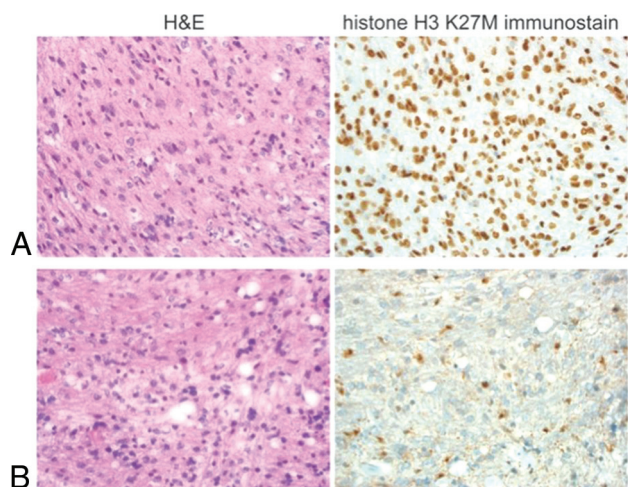


FIG 1. Histology of H3-K27M and wild-type diffuse midline gliomas. Hematoxylin and eosin (H&E) and antihistone H3-K27M immunohistochemistry of diffuse intrinsic pontine gliomas with H3-K27M mutation (A) and histone H3 wildtype (B). 400x magnification.

coregistration. Voxel-based ADC values were extracted, and a range of ADC values was generated for each patient.

Data Analysis

Histogram descriptive statistics were calculated using STATA SE, 14.1 2016 (StataCorp, College Station, Texas) and included mean, median, minimum, maximum, and percentiles (5th to 95th in increments of 5, 1st percentile, and 99th percentile). Comparative analysis of histogram descriptive statistics between histone H3-K27M mutant and wild-type diffuse midline gliomas was performed using standardized Student *t* tests. Kaplan-Meier survival analysis was completed in patient subgroups on the basis of the presence of the histone H3-K27M mutation and an ADC below 1.1×10^{-3} mm²/s.

RESULTS

Forty-four pediatric patients with diffuse gliomas were initially identified on retrospective chart review (Table). Thirty-one patients had diffuse midline gliomas and met all inclusion criteria necessary for analysis. Twenty-one patients (68%) had infratentorial tumors located within the pons, vermis, or fourth ventricle. Independent testing for the presence of the histone H3-K27M mutant protein by immunohistochemistry within these tumors was available in all patients. Twenty-three patients (73%) carried

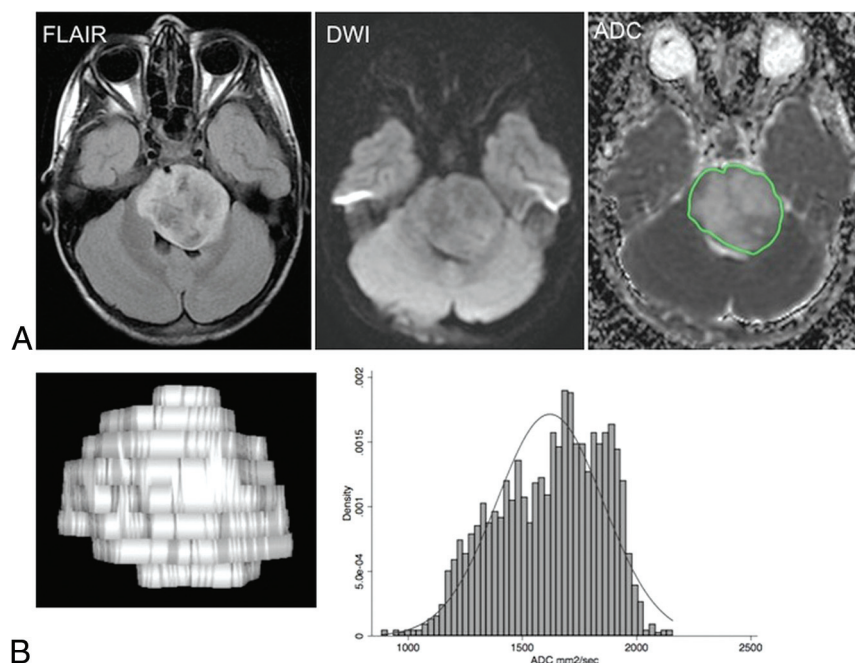


FIG 2. Diffusion characteristics of diffuse midline gliomas based on the presence of the H3-K27M mutation. Tumor 3D volume segmented from the FLAIR image (A) was coregistered onto the ADC map. Voxel-based histogram of tumor (B). Normal distribution curves are superimposed on the ADC histograms.

histone H3-K27M mutations. Tumors carrying histone H3-K27M mutations showed positive nuclear staining with the anti-H3-K27M antibody (Fig 1).

Tumor segmentation was performed, and an ROI was manually drawn (Fig 2). Distribution of ADC values per voxel within the segmented tumor was displayed as a histogram (Fig 2B) and descriptive statistics, including percentile values, variance, skewness, and kurtosis. There were no statistically significant differences in ADC mean, median, minimum, and percentile values between histone H3-K27M mutant and wild-type tumors (Fig 3 and On-line Table 1). There were also no statistically significant differences in variance, skewness, or kurtosis of the histograms between H3-K27M mutant and wild type tumors (Fig 4). Representative images of patients with positive and negative skewness and high and low kurtosis are demonstrated in Fig 4B.

ADC histogram characteristics of diffuse midline gliomas were compared with 5 hemispheric glioblastomas that were present within our cohort, which were all histone H3 wild-type. The midline gliomas had higher mean and median ADC values compared with hemispheric glioblastomas ($P < .05$; Fig 5). The ADC mean for diffuse midline gliomas was $1.28 \times 10^{-3} \text{ mm}^2/\text{s}$ (95% CI, 1.21–1.34) and $0.86 \times 10^{-3} \text{ mm}^2/\text{s}$ (95% CI, 0.69–1.01) for hemispheric glioblastomas ($P < .05$).

Clinical outcomes at 12 months after diagnostic biopsy were available in 19 patients. Thirteen patients were alive at 12 months after biopsy. Among patients with histone H3-K27M mutant tumors ($n = 15$), nine were alive at 12 months after diagnostic biopsy. Among patients with wild-type diffuse midline gliomas ($n = 6$), five had follow-up with only 2 patients alive at 12 months after biopsy.

Kaplan-Meier curves demonstrated that survival was worse in patients with histone H3-K27M mutated tumors (Fig 6A). Statistically significant higher mean and median ADC values were found in patients who survived longer than 12 months compared with those who died within 12 months of biopsy (On-line Table 2). Kaplan-Meier survival comparison of patients segregated on the basis of the ADC cutoff value of $1.1 \times 10^{-3} \text{ mm}^2/\text{s}$ demonstrated that patients with lower ADC values had worse survival. The ADC cutoff was determined using receiver operating characteristic curve analysis for prediction of survival after 12 months, which identified a cutoff of $1.18 \times 10^{-3} \text{ mm}^2/\text{s}$. There were 8 patients with ADC values below $1.1 \times 10^{-3} \text{ mm}^2/\text{s}$, 5 of whom had a mutation for histone H3-K27M and 3 of whom had wild-type tumors. There were 23 patients with elevated ADC values, with 18 patients having the histone H3-K27M mutation and

5 having wild-type tumors. For evaluating mutations beyond histone H3-K27M, gene panel testing of 500 cancer genes was available in only 1 patient from the decreased diffusivity group ($\text{ADC} < 1.1 \times 10^{-3} \text{ mm}^2/\text{s}$), which revealed somatic mutations in histone H3-K27M, *PIK3CA*, and *PPM1D* genes, and gain of chromosome 1q. On the other hand, 2 of the patients with elevated ADC were tested with the cancer gene panel demonstrating mutations in *TP53*, *BCORL1*, *PDGFRA*, *PIK3CA*, and *ASXL1*, with both of the tumors carrying the *TP53* mutation.

DISCUSSION

Pediatric diffuse midline gliomas tend to be refractory to treatment and carry some of the poorest prognoses of all pediatric cancers. Yet, even within this group, there is some variability in outcome. Diffuse midline gliomas carrying histone H3-K27M mutations appear to represent the worst prognosis. It is challenging to identify these tumors on the basis of imaging, and to date, no reliable imaging characteristics have been found to delineate histone H3-K27M mutant gliomas from wild-type diffuse midline gliomas.⁵ We previously described the qualitative characteristics of these diffuse midline gliomas with the histone H3-K27M mutation, including patterns of enhancement, necrosis, and infiltrative appearance. Unfortunately, none of these qualitative characteristics could distinguish the K27M mutant tumors from wild-type tumors. In the current article, we evaluated the diffusion characteristics of diffuse midline gliomas based on clinical DWI imaging and ADC histogram analysis.

In our study, ADC histogram analysis of diffuse midline gliomas did not demonstrate statistically significant differences in mean, median, minimum, maximum, and percentile ADC values between histone H3-K27M mutant and wild-type tumors, nor

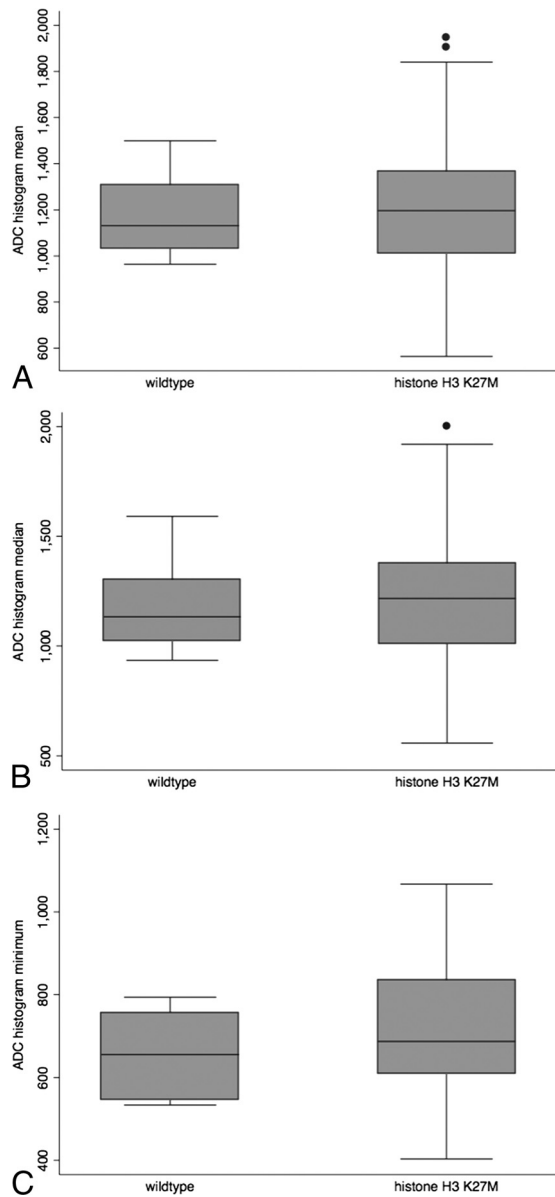


FIG 3. Voxel-based 3D whole-tumor ADC boxplots comparing histone H3-K27M and wild-type tumors without a difference in ADC_{mean} (A), ADC_{median} (B), and ADC_{min} ($10^{-6}\text{mm}^2/\text{s}$) (C).

did it demonstrate differences in variance, kurtosis, or skewness of the comparison histograms. These findings suggest that diffuse midline gliomas are architecturally very similar, despite molecular differences in the presence or absence of histone H3-K27M mutations. Given that tumors with histone H3-K27M mutations are known to carry worse outcomes than wild-type tumors,^{4,11} we remain hopeful that there may be more advanced imaging markers that can help delineate these tumors on imaging such as advanced imaging postprocessing and metabolic imaging with MR spectroscopy.

Our study did reveal that pediatric diffuse midline gliomas have overall ADC values with a mean of $1.4 \times 10^{-3}\text{mm}^2/\text{s}$. This was statistically significantly higher than infiltrative glioblastomas located within the cerebral hemisphere, suggesting a different cellular architecture within these tumors. We anticipate that the

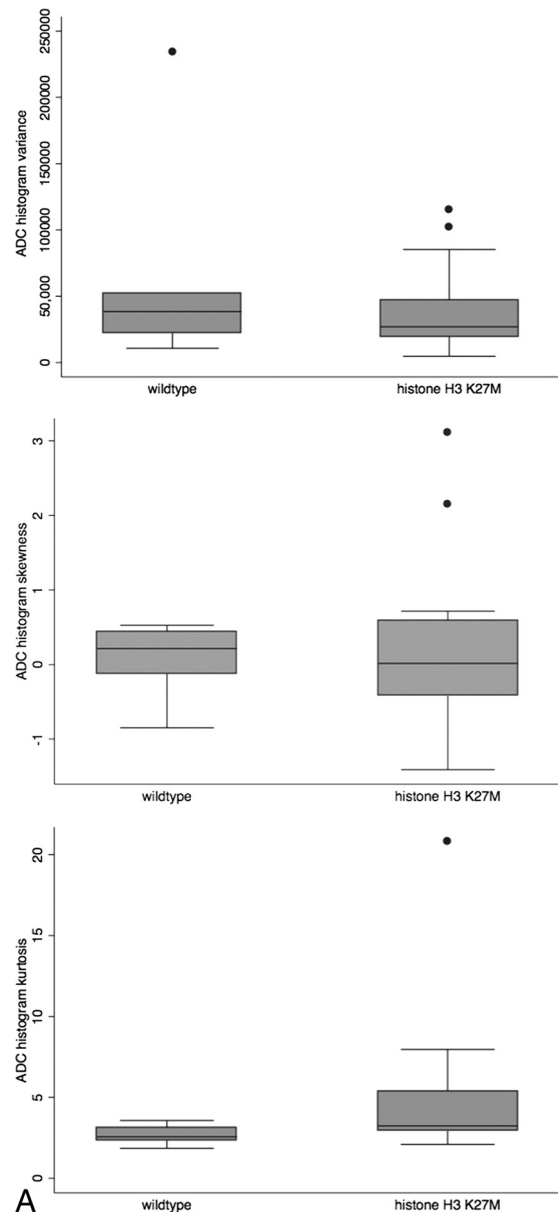


FIG 4. ADC histogram descriptive statistics of diffuse midline gliomas. No difference in skewness, kurtosis, and variance between wild-type and histone H3-K27M mutant tumors (A). Examples of histogram parameters of ADC ($10^{-6}\text{mm}^2/\text{s}$) (B). Normal distribution curves are superimposed on the ADC histograms. (Continued on next page)

infiltrative cellular organization in midline gliomas leads to increased diffusivity, while tight cellular architecture within hemispheric glioblastomas results in reduced diffusivity on DWI sequences. Further studies with larger patient numbers need to be performed.

One notable finding that our study demonstrated was that patients with lower ADC values had lower survival rates at 12 months than patients with ADC values higher than 1.1. This finding agrees with a previous report showing that lower ADC values in a group of diffuse intrinsic pontine glioma tumors correlated with worse patient outcomes.¹² The combination of these findings suggests that a lower ADC within diffuse midline gliomas is an independent imaging marker of

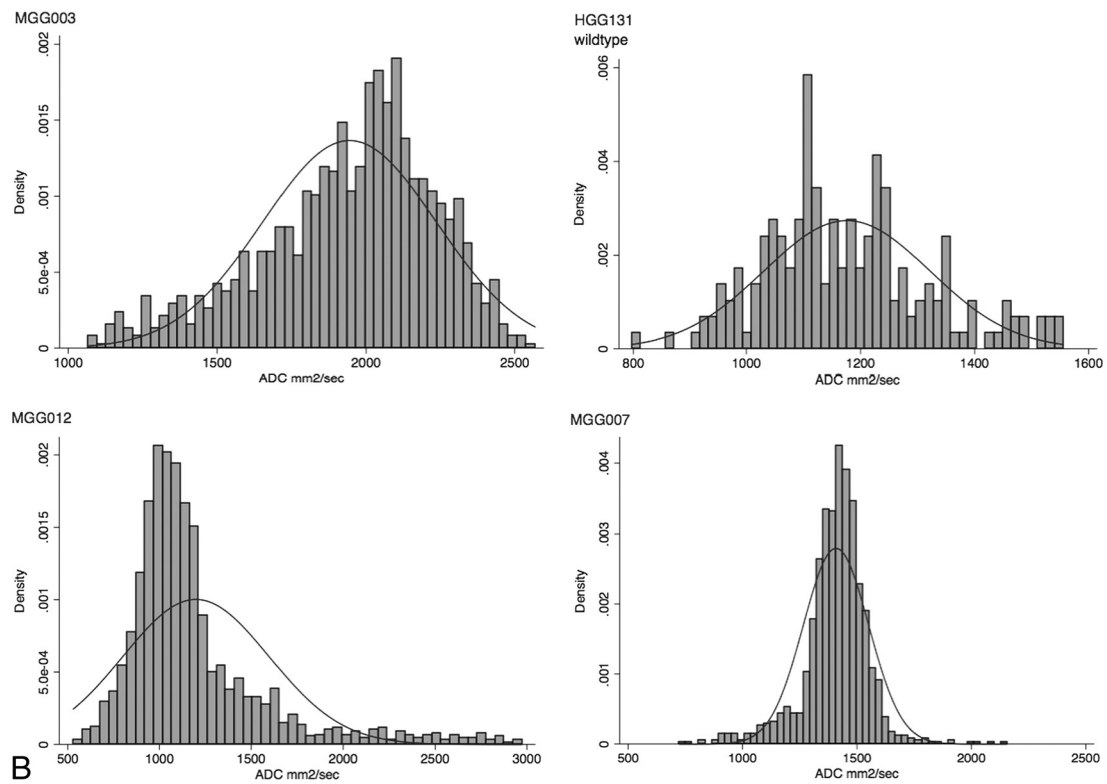


FIG 4. Continued.

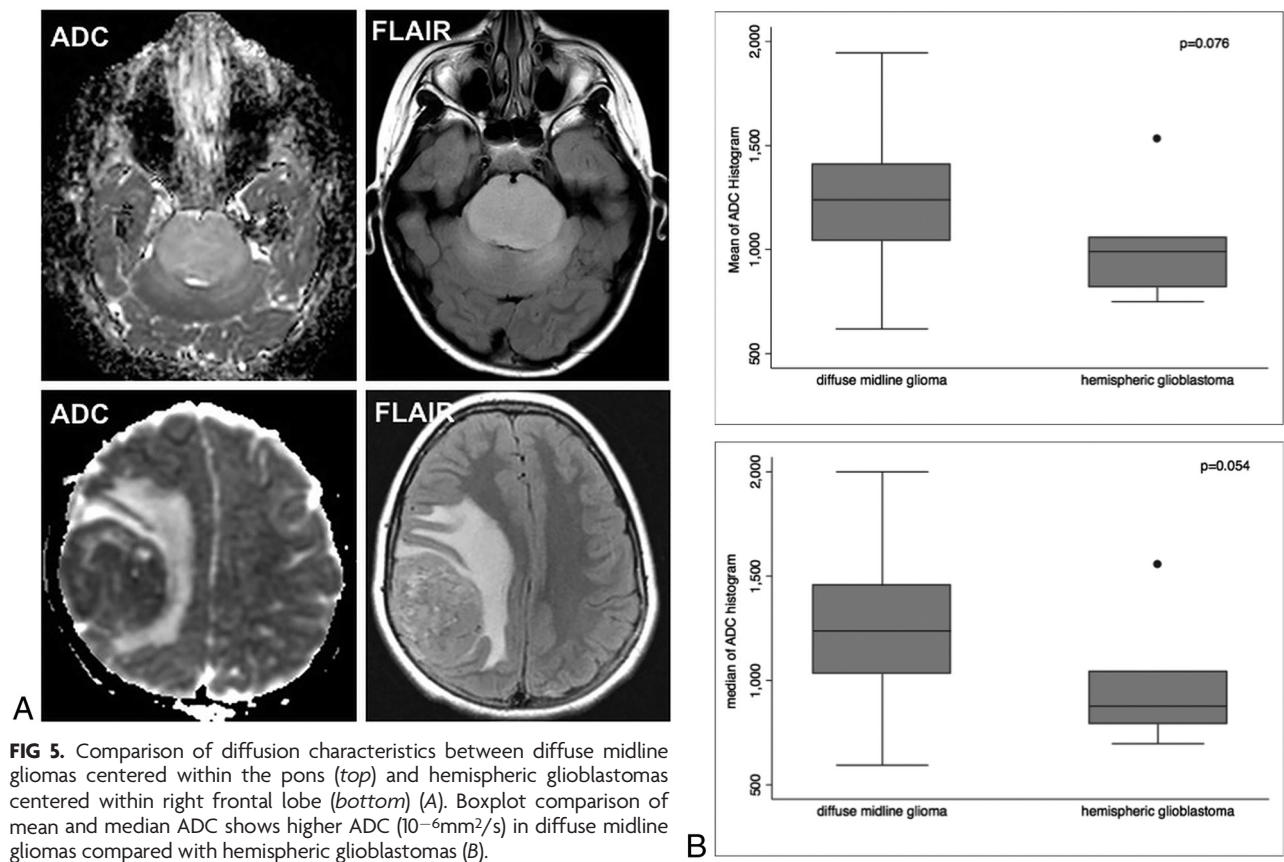


FIG 5. Comparison of diffusion characteristics between diffuse midline gliomas centered within the pons (*top*) and hemispheric glioblastomas centered within right frontal lobe (*bottom*) (A). Boxplot comparison of mean and median ADC shows higher ADC (10⁻⁶mm²/s) in diffuse midline gliomas compared with hemispheric glioblastomas (B).

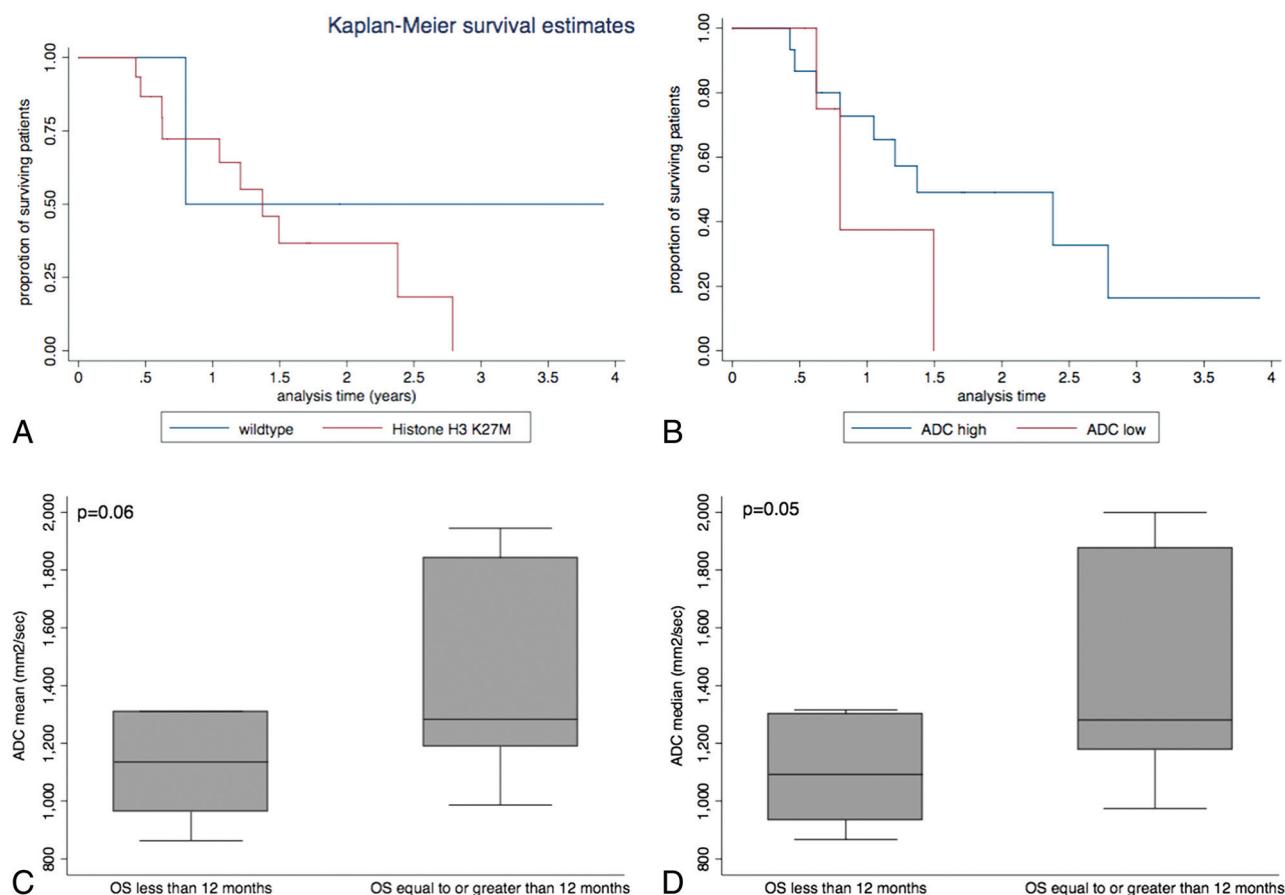


FIG 6. Kaplan-Meier survival curve based on histone H3-K27M mutation status (A) and ADC (10^{-6} mm²/s) being below the 1.1×10^{-3} mm²/s cut-off (B). Boxplots of ADC mean and median comparing patients with overall survival <12 months and ≥ 12 months (C and D).

worse outcomes, perhaps even independent of the H3-K27M mutation. This also suggests the need for differentiation of histone H3.1 and H3.3 K27M mutations in clinical samples because standard of care clinical evaluation of these tumors involves immunohistochemistry staining with an antibody that detects both H3.1 and H3.3 histone subtypes. Prior studies demonstrated that patients with histone H3.3 K27M mutant tumors had worse overall survival compared with those with H3.1 tumors; thus, it is important to evaluate the diffusivity in patients having histone H3.3 and H3.1 mutations.³ In our study, we had a small subset of patients who had the 500 Cancer Gene Panel Test with 1 patient tested in the low-ADC group and 2 patients tested in the high-ADC group. Both patients in the high-ADC group had mutations in the *TP52* gene, while the patient in the low-ADC group had mutations previously described in diffuse midline gliomas, *PIK3CA* and *PPM1D*.¹³ Further detailed genetic analysis of these subgroups based on tumor diffusion characteristics may identify the genes that influence patient outcomes and may identify new therapeutic targets.

CONCLUSIONS

Although no statistically significant difference in diffusion characteristics is found between histone H3-K27M mutant and wild-type midline tumors, lower diffusivity corresponds to a lower

survival rate at 1 year after diagnosis. These findings can have an impact on the anticipated clinical course for this patient population and offer providers and families guidance on clinical outcomes.

Disclosures: Cassie Kline—*UNRELATED: Grant:* Cannonball Kids' Cancer Foundation, Frank A. Campini Foundation, University of California, San Francisco School of Medicine Dean's Diversity Award. Elizabeth Tong—*RELATED: Grant:* National Institutes of Health T32 Grant. Caroline Jordan—*RELATED: Grant:* National Institutes of Health. Steve Braunstein—*UNRELATED: Employment:* University of California, San Francisco, *Comments:* Faculty Radiation Oncologist. Sabine Mueller—*RELATED: Grant:* Clinical and Translational Science KL2 Award, *Comments:* The National Center for Advancing Translational Sciences, National Institutes of Health, through the University of California, San Francisco—Clinical and Translational Science Institute Grant No. KL2TR000143.

REFERENCES

- Hoshida R, Jandial R. 2016 World Health Organization Classification of Central Nervous System Tumors: an era of molecular biology. *World Neurosurg* 2016;94:561–62 CrossRef Medline
- Solomon DA, Wood MD, Tihan T, et al. Diffuse midline gliomas with H3-K27M mutation: a series of 47 cases assessing the spectrum of morphologic variation and associated genetic alterations. *Brain Pathol* 2016;26:569–80 CrossRef Medline
- Castel D, Philippe C, Calmon R, et al. Histone H3F3A and HIST1H3B K27M mutations define two subgroups of diffuse intrinsic pontine gliomas with different prognosis and phenotypes. *Acta Neuropathol* 2015;130:815–27 CrossRef Medline
- Korshunov A, Ryzhova M, Hovestadt V, et al. Integrated analysis of pediatric glioblastoma reveals a subset of biologically favorable

- tumors with associated molecular prognostic markers. *Acta Neuropathol* 2015;129:669–78 CrossRef Medline
5. Aboian MS, Solomon DA, Felton E, et al. **Imaging characteristics of pediatric diffuse midline gliomas with histone mutation.** *AJNR Am J Neuroradiol* 2017;38:795–800 CrossRef Medline
 6. Rodriguez Gutierrez D, Awwad A, Meijer L, et al. **Metrics and textural features of MRI diffusion to improve classification of pediatric posterior fossa tumors.** *AJNR Am J Neuroradiol* 2014;35:1009–15 CrossRef Medline
 7. Bull JG, Saunders DE, Clark CA, et al. **Discrimination of paediatric brain tumours using apparent diffusion coefficient histograms.** *Eur Radiol* 2012;22:447–57 CrossRef Medline
 8. Nowosielski M, Recheis W, Goebel G, et al. **ADC histograms predict response to anti-angiogenic therapy in patients with recurrent high-grade glioma.** *Neuroradiology* 2011;53:291–302 CrossRef Medline
 9. Pope WB, Lai A, Mehta R, et al. **Apparent diffusion coefficient histogram analysis stratifies progression-free survival in newly diagnosed bevacizumab-treated glioblastoma.** *AJNR Am J Neuroradiol* 2011;32:882–89 CrossRef Medline
 10. Pope WB, Kim HJ, Huo J, et al. **Recurrent glioblastoma multiforme: ADC histogram analysis predicts response to bevacizumab treatment.** *Radiology* 2009;252:182–89 CrossRef Medline
 11. Sturm D, Witt H, Hovestadt V, et al. **Hotspot mutations in H3F3A and IDH1 define distinct epigenetic and biological subgroups of glioblastoma.** *Cancer Cell* 2012;22:425–37 CrossRef Medline
 12. Poussaint TY, Vajapeyam S, Ricci KI, et al. **Apparent diffusion coefficient histogram metrics correlate with survival in diffuse intrinsic pontine glioma: a report from the Pediatric Brain Tumor Consortium.** *Neuro Oncol* 2016;18:725–34 CrossRef Medline
 13. Nikbakht H, Panditharatna E, Mikael LG, et al. **Spatial and temporal homogeneity of driver mutations in diffuse intrinsic pontine glioma.** *Nat Commun* 2016;7:11185 CrossRef Medline